

## Supporting Information for

Photodynamic Therapy Using Hybrid Nanoparticles Comprising Upconversion Nanoparticle and Chlorin e6-bearing Pullulan

Riku Kawasaki,<sup>\*,‡</sup> Takuro Eto,<sup>‡</sup> Nanami Kono, Reo Ohdake, Keita Yamana, Shogo Kawamura, Hidetoshi Hirano, Naoki Tarutani, Kiyofumi Katagiri, and Atsushi Ikeda\*

Applied Chemistry Program, Graduate School of Advanced Science and Engineering, Hiroshima University, 1-4-1 Kagamiyama, Higashi-Hiroshima, 739-8527, Japan

### Table of contents

Materials and Methods	2-5
Scheme S1 and Fig. S1	6
Fig. S2 and S3	7
Fig. S4, S5, and S6	8
Fig. S7 and Table S1	9
Fig. S8, S9 and Scheme S2	10
Fig. S10 and S11	11
Fig. S12 and S13	12
Fig. S14, S15 and S16	13
Fig. S17 and S18	14
Fig. S19 and S20	15
Fig. S21 and S22	16
Fig. S23 and S24	17
Fig. S25 and S26	18
Fig. S27	19

## **Materials and Methods**

### **Materials and animals**

Pullulan was purchased from Tokyo Chemical Industry Corporation (Tokyo, Japan). Chlorin e6 was purchased from Santa Cruz Biotechnology (Texas, USA). Dimethyl sulfoxide (DMSO), tetrahydrofuran (THF), *N,N'*-dicyclohexylcarbodiimide (DCC) and *N,N*-dimethyl-4-aminopyridine (DMAP) were purchased from FUJIFILM Wako Pure Chemical Corporation (Tokyo, Japan). Rare earth doped upconversion nanoparticles and 9,10-anthracenediyl-bis(methylene)-dimalonic acid (ABDA) were purchased from Sigma Aldrich (Missouri, USA). Murine colon cancer (colon26), Mouse fibroblasts (L929) were kindly given by Prof. Takeshi Nagasaki (Osaka Metropolitan University) and Prof. Alexandra Stubelius (Chalmers University of Technology). These cell lines were maintained in Dulbecco's Eagle Medium (Thermo Fischer Science, Massachusetts, USA) containing fetal bovine serum (Thermo Fischer Science) and anti-anti. Balb/c mouse were purchased from Japan SLC (Shizuoka, Japan). All the animal experiments were approved the animal experiment ethic committee in Hiroshima University (C22-40).

### **Synthetic of chlorin e6 bearing pullulan**

Pullulan (0.20 mmol) was dissolved in DMSO at 40 °C for 1 h with stirring. Pullulan was then purified by dialysis (MWCD, 8 kD) in water for 3 days and lyophilization. *N,N*-dicyclohexylcarboimide (DCC), chlorin e6 (dissolved in DMSO), and 1.0 mL of a dry DMSO solution of *N,N*-dimethyl-4-aminopyridine (DMAP) were added and stirred at 45 °C for 2 days under shielded light. The resulting solution was purified in DMSO for 1 day (MWCD, 8 kD) and in water for 2 days (MWCD, 8 kD). Finally, the chlorin e6-bearing pullulan was obtained by lyophilization. These samples were analyzed using <sup>1</sup>H-NMR (Varian 500 MHz, Agilent Technologies, Santa Clara, CA, USA) and Ultraviolet-Visible light absorption spectrum measurement (3600 UV-vis-NIR spectrometers; Shimadzu, Tokyo, Japan).

### **Nanoparticle formulation**

Chlorin e6-bearing pullulan (1 mg) was stirred in milliQ (1 mL) overnight to dissolve all polymers completely. Then, nanoparticles were prepared by sonication (TOMY, Tokyo, Japan) in ice water for 30 minutes. The nanogel formation was confirmed by dynamic light scattering (DLS) measurement (Zetasizer Nano ZS; Malvern, Malvern, UK) and transmission electron microscopy (TEM, JEM-1400 field emission electron microscope; JEOL Ltd., Tokyo, Japan). The samples were observed with staining reagents (4% phosphotungstic acid). Acceleration voltage was set at 100 kV.

### **Hybrid nanoparticles formulation**

Hybrid nanoparticles were prepared by complexing water dispersion solutions (1.0 mg•mL<sup>-1</sup>, 1.0 mL) of the nanoparticles with THF dispersion solutions (1, 10, 100 µg•mL<sup>-1</sup>, 100 µL) of UCNPs by injection. The hybrid formulation was confirmed by DLS and TEM. In case with TEM, the samples were observed without staining reagents.

### **Singlet oxygen species generation** □

Singlet oxygen generation was measured by the ABDA bleaching method. Singlet oxygen produced by near-infrared light irradiation was evaluated by the decrease in absorbance of 9,10-anthracenediyl-bis(methylene)dimaronic acid (ABDA), an anthracene derivative, due to singlet oxygen generation. The UV cell was filled with 2670 µL of milliQ and oxygen bubbled for 30 minutes. Aqueous dispersion solution of hybrid nanogel (1.0mg•mL<sup>-1</sup>, 300 µL) was added and it was used as blank. The ABDA stock solution in DMSO (ABDA, 2.5 µM; 30µL) was added to the aqueous dispersion of hybrid nanogels, irradiated with near-infrared light (980 nm), and UV-vis absorption spectra were measured at 0, 7.5, 15, 30, and 60 minutes.

### **Cytotoxicity of cancer cell lines and fibroblast cell lines cells by Che6P-UCNPs**

Colon26 and L929 cells were seeds on 96-well plates at 5,000 cell/well and incubated overnight. Cells were exposed to various concentrations of nanogels in aqueous media under shading for 24h. Then, the cell counting kit was used to count cells. Absorbance at 450 nm was measured to determine cell viability using microplate reader (ASONE).

### **Photodynamic activity against cancer cell lines and fibroblast cell lines**

Colon26 and L929 cells were seeded on 48-well plates at 1.71×10<sup>4</sup> cells/well and incubated overnight. Cells were exposed to various concentrations of Che6P-UCNPs in aqueous media for 24 h. After exchanging the medium, cells were irradiated with near-infrared light (980 nm) for 30 min. Cells were additionally incubated for 24 h. Then, the cell counting kit was used to quantify the number of living cells. Absorbance at 450 nm was measured to determine cell viability.

### **Subcellular distribution of Che6P-UCNPs**

Colon26 cells were seeded on glass-bottom dishes at 1.0×10<sup>5</sup> cells and incubated overnight. Cells were exposed to hybrid nanoparticles at 100 µg•mL<sup>-1</sup> for 24h. Then, cells were washed with PBS and the cells were observed by confocal laser scanning microscope (LSM700, Carl Zeiss, Germany).

### **Fluorescence-activated cell sorting** □

Colon26 cells were seeded on 12-well plates at  $1.0 \times 10^5$  cell/well and incubated overnight. Cells were exposed to hybrid nanogels at  $100 \mu\text{g} \cdot \text{mL}^{-1}$  for 24h. Then, cells were washed with PBS and added Trypsin-EDTA. Finally, the samples were resuspended in PBS and the cellular uptake amount was analyzed by flow cytometry (FACS Calibur; Becton Dickinson, New Jersey, USA).

### **Spheroid preparation**

Colon26 cells were seeded on EZ sphere for spheroid formation at 19,000 cell/well and incubated overnight. The grown spheroids were transferred to 12-well plates and hybrid nanogels were added.

### **Distribution of the hybrid in spheroids**

Spheroids were exposed to  $100 \mu\text{g} \cdot \text{mL}^{-1}$  nanogels and  $33.1 \mu\text{M}$  Photofrin for 24 h. Then, cells were washed with PBS. 4% paraformaldehyde was added for fixation. After treatment with 0.1% Triton-X, the nuclei were stained by DAPI. The samples were observed by confocal laser scanning microscope.

### **Spheroid growth inhibitory effects through photodynamic activity**

Spheroids were exposed to  $100 \mu\text{g} \cdot \text{mL}^{-1}$  hybrid nanoparticles for 24 h. After exchanging medium, cells were near infrared light irradiated for 30 min. Spheroidal volume was measured at each time point (0, 1, 2, and 4 h). Spheroid volumes were calculated using the following equation (1).

$$V = \pi(\text{long axis}) \times (\text{short axis})^2 / 2 \quad (1)$$

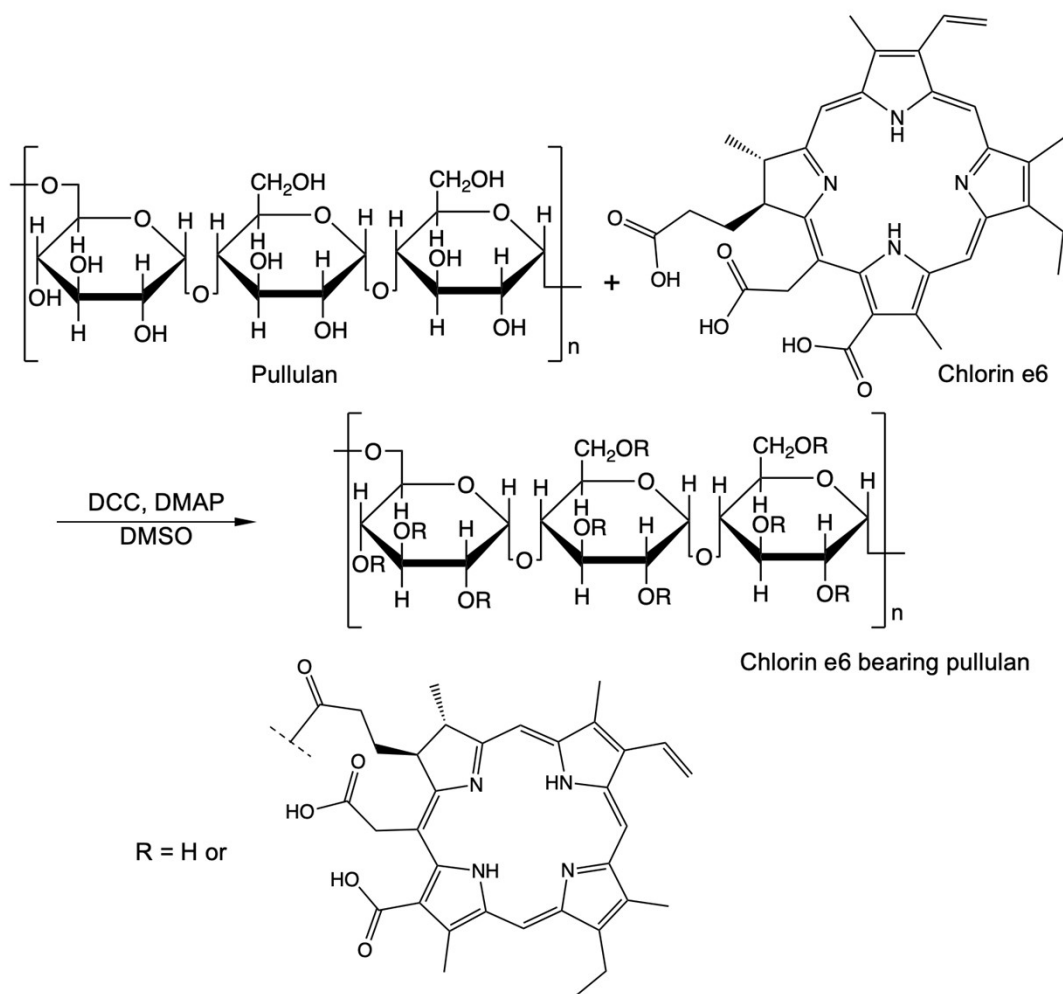
### **Pharmacokinetic study of the hybrid in tumor xenograft mice**

Suspension of Colon26 cells ( $5.0 \times 10^5$  cells) were injected to right femur of Balb/c mice (4-week-old, male, 18 g) *via* subcutaneous injection. When the tumor volume reached approximately  $80 \text{ mm}^3$ , dispersion of Che6P-0.54-UCNPs-100 ( $1 \text{ mg} \cdot \text{mL}^{-1}$ ,  $100 \mu\text{L}$ ) were intravenously injected. At each time point (0, 1, 3, 6, and 24 h), blood was collected with Goldenrod and accumulation was monitored by *in vivo* imaging system (NightOWL). At 24 h post injection, accumulation in each organ (tumor, liver, lung, heart, kidney, and spleen) was visualized by NightOWL. Accumulation of Che6P-0.54-UCNPs-100 in organs (tumor, liver, lung, heart, kidney, spleen, and blood) was quantified by ICP-AES after digestion of organs using aqua regia. Intratumoral distribution of Che6P-0.54-UCNPs-100 were observed by CLSM after nuclei staining using DAPI.

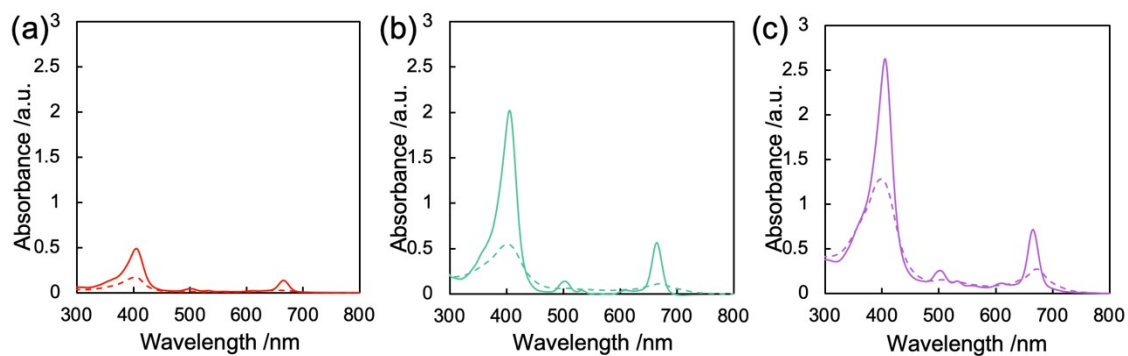
### **NIR-triggered PDT in tumor xenograft mice using Che6P-0.54-UCNPs-100**

Suspension of Colon26 cells ( $5.0 \times 10^5$  cells) were injected to right femur of Balb/c mice (4-week-old, male, 18 g) *via* subcutaneous injection. When the tumor volume reached approximately  $80 \text{ mm}^3$ , dispersion of Che6P-0.54-UCNPs-100 ( $1 \text{ mg}\cdot\text{mL}^{-1}$ ,  $100 \text{ }\mu\text{L}$ ) were intravenously injected. After 24 h incubation, NIR laser was irradiated to tumor tissue for 1 h. At each time point, tumor size were measured and their size were determined by following equation (1).

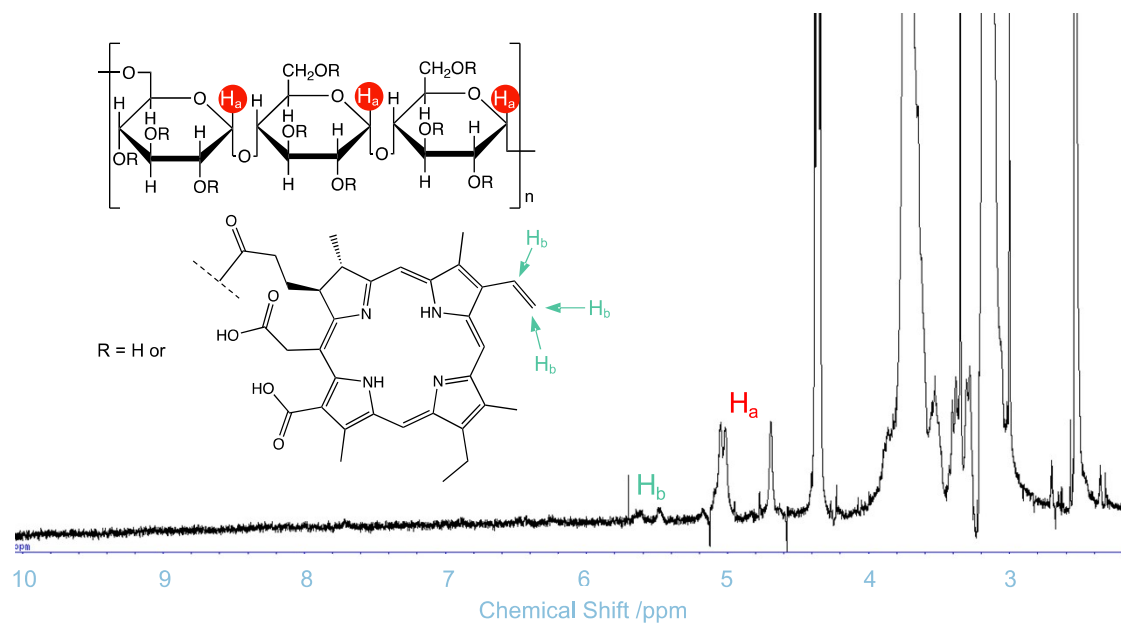
At the end point, each organ (tumor, liver, lung, heart, kidney, and spleen) was isolated and fixed with 4 % paraformaldehyde. Metastatic tumor in lung was counted to score the metastasis inhibition. To quantify the retention in each organ was monitored by ICP-AES after digestion with aqua regia.



**Scheme S1** Synthetic route of chlorin e6 bearing pullulan

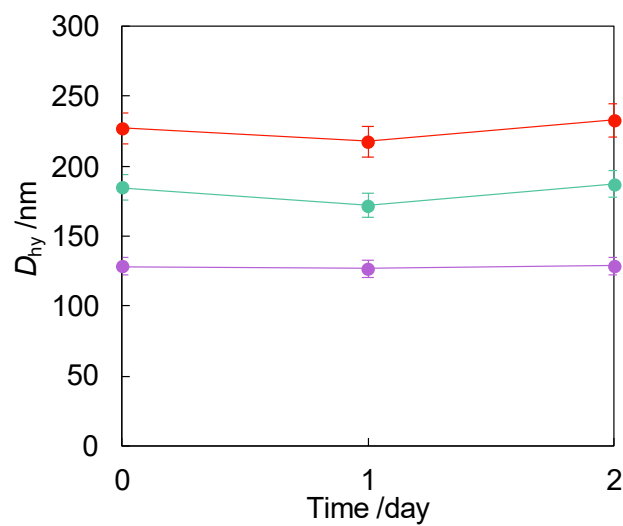


**Fig. S1** Absorption spectra of Che6P and Che6P nanogel. Che6P-0.54 (a), Che6P-2.22 (b), and Che6P-2.80 (c) were dissolved in DMSO at  $1 \text{ mg}\cdot\text{mL}^{-1}$  (solid line). Che6P nanogels were prepared at  $1 \text{ mg}\cdot\text{mL}^{-1}$  in aqueous media (dashed line).

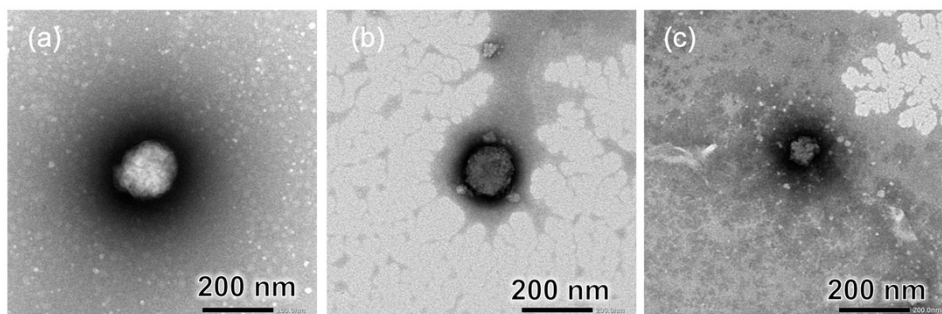


**Fig. S2**  $^1\text{H}$  NMR spectra of Che6P-2.80. The samples were prepared in the mixture of  $\text{d}_6$ -DMSO and  $\text{D}_2\text{O}$  (9 : 1, v/v).

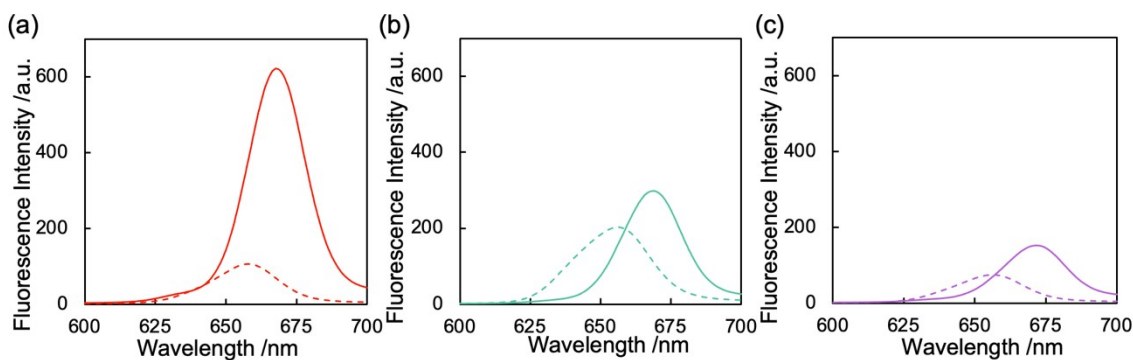
(a) anomeric proton in pullulan and (b) acrylic proton.



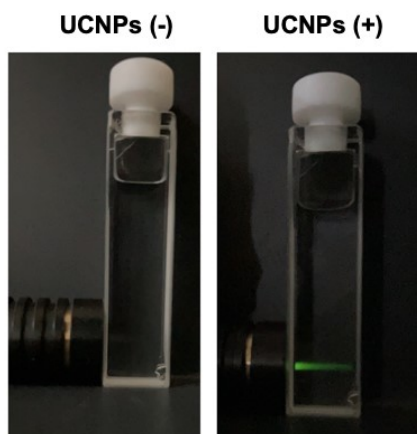
**Fig. S3** Changes in hydrodynamic diameter ( $D_{\text{hy}}$ ) of Che6P nanogel in aqueous media. Che6P-0.54 (red), Che6P-2.22 (blue), and Che6P-2.80 (purple).



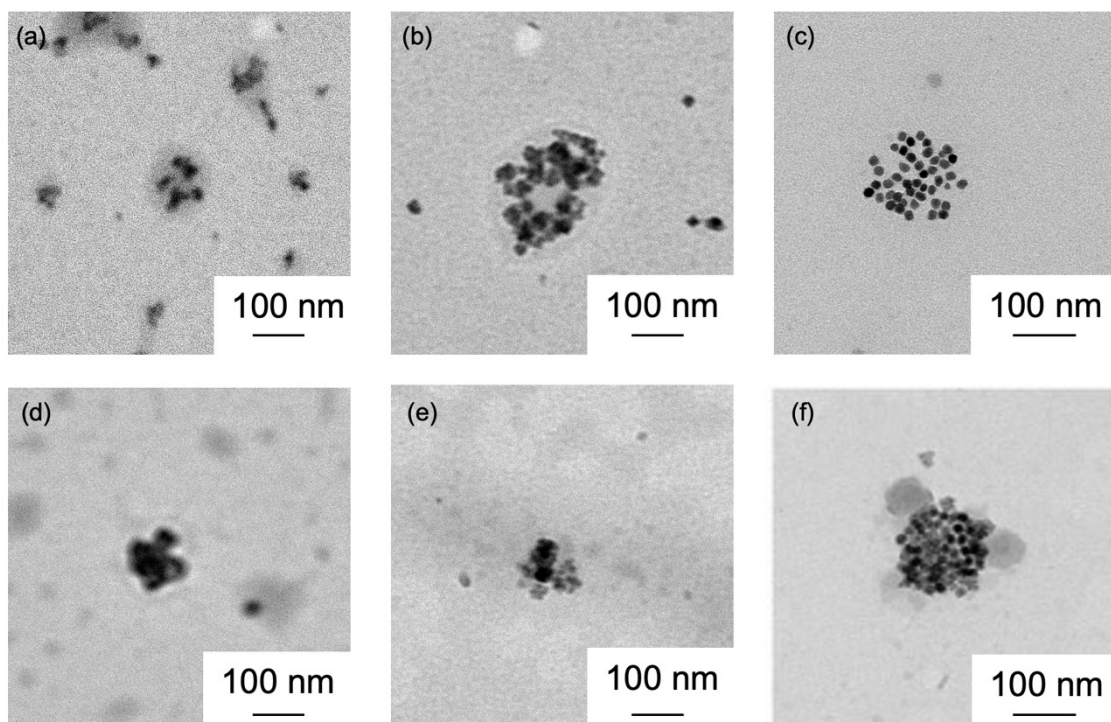
**Fig. S4** Representative morphological images of Che6P nanogel (a, Che6P-0.54; b, Che6P-2.22; c, Che6P-2.80). The samples were stained with 4% phosphotungstic acid. (Acceleration voltage, 100 kV)



**Fig. S5** Fluorescence spectra of Che6P and Che6P nanogel. Che6P-0.54 (a), Che6P-2.22 (b), and Che6P-2.80 (c) were dissolved in DMSO at  $1 \text{ mg}\cdot\text{mL}^{-1}$  (solid line). Che6P nanogels were prepared at  $1 \text{ mg}\cdot\text{mL}^{-1}$  in aqueous media (dashed line). The samples were excited at 400 nm.



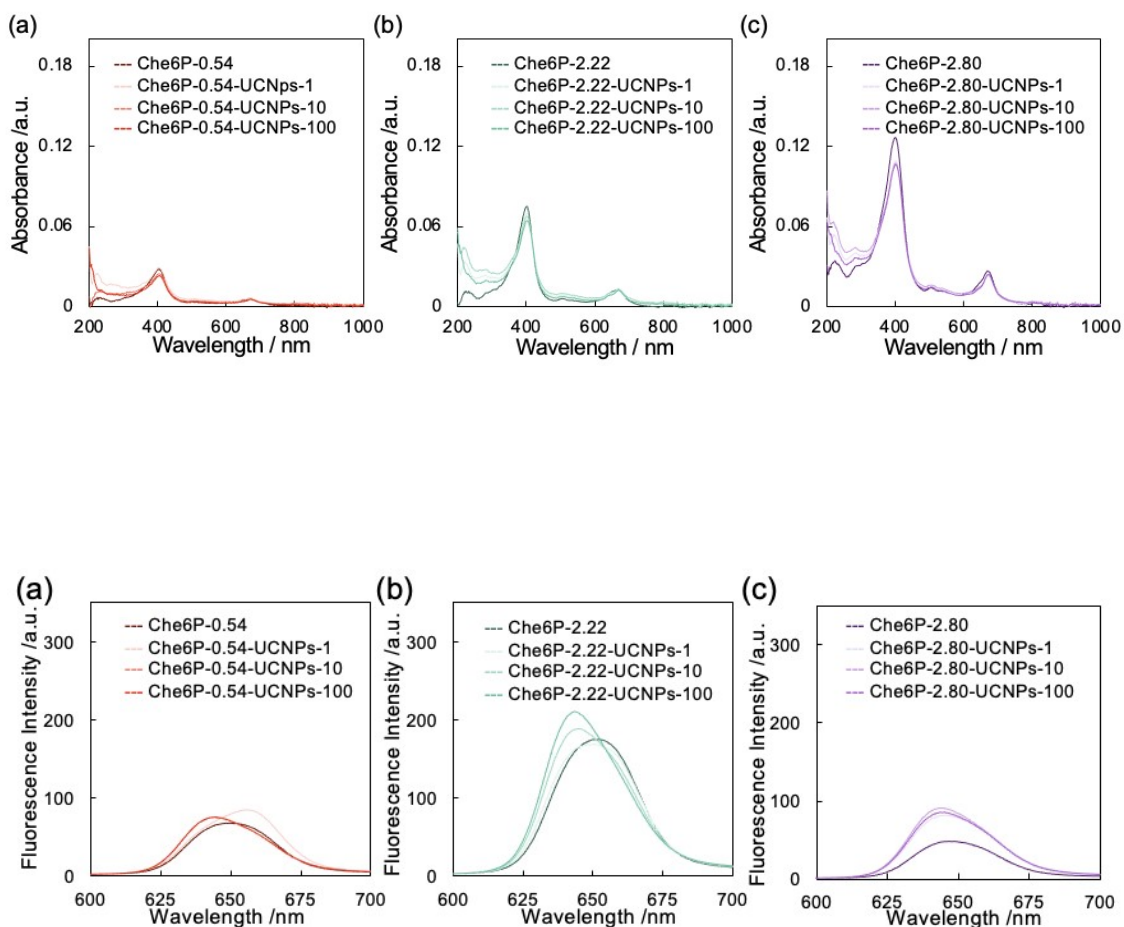
**Fig. S6** Digital photograph of 980 nm laser emitted UCNPs dispersion.



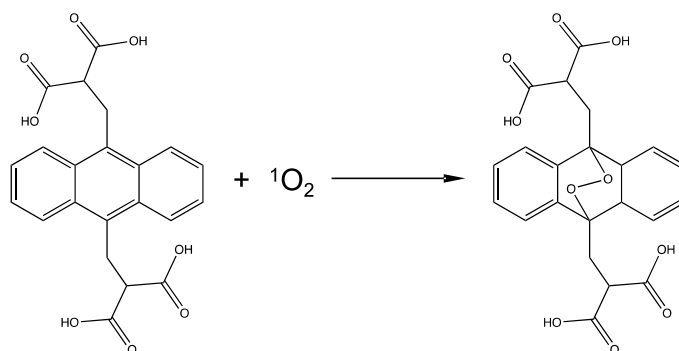
**Fig. S7** Representative morphology of Che6P-UCNPs. (a) Che6P-2.22-UCNPs-1, (b) Che6P-2.22-UCNPs-10, (c) Che6P-2.22-UCNPs-100, (d) Che6P-2.80-UCNPs-1, (e) Che6P-2.80-UCNPs-10, (f) Che6P-2.80-UCNPs-100 (Acceleration voltage, 100 kV)

**Table S1** Number of UCNPs in each nanoparticle

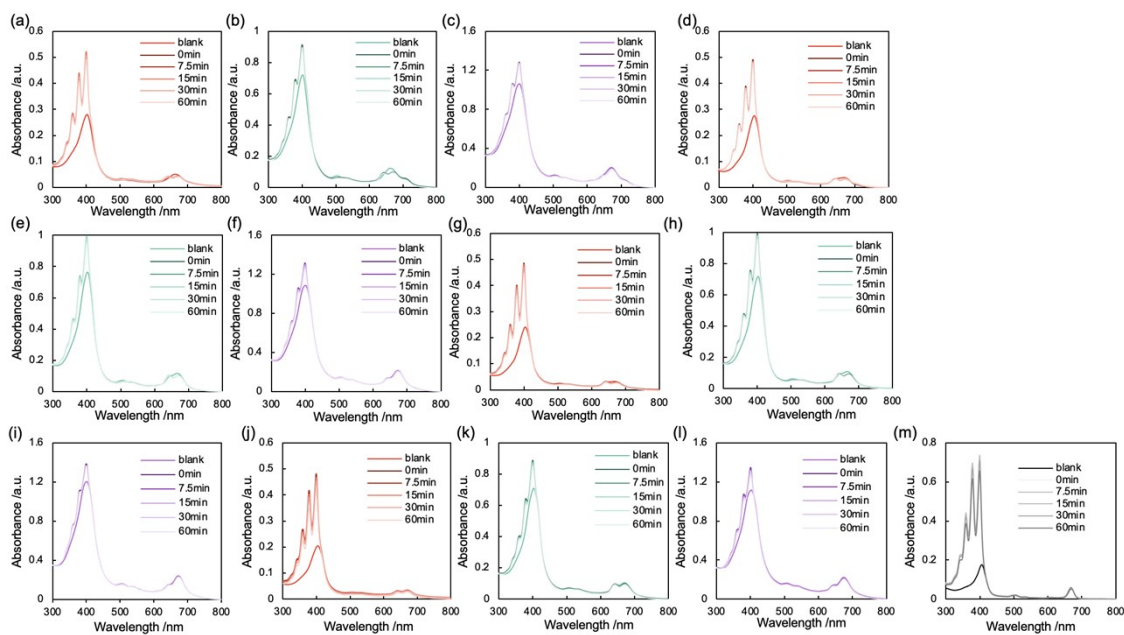
	Number of UCNPs
Che6P-0.54-UCNPs-1	$2.7 \pm 1.6$
Che6P-0.54-UCNPs-10	$17.9 \pm 5.7$
Che6P-0.54-UCNPs-100	$47.5 \pm 9.8$
Che6P-2.22-UCNPs-1	$2.9 \pm 1.9$
Che6P-2.22-UCNPs-10	$15.8 \pm 7.6$
Che6P-2.22-UCNPs-100	$42.8 \pm 16.6$
Che6P-2.80-UCNPs-1	$2.6 \pm 1.9$
Che6P-2.80-UCNPs-10	$17.3 \pm 5.0$
Che6P-2.80-UCNPs-100	$37.2 \pm 7.9$



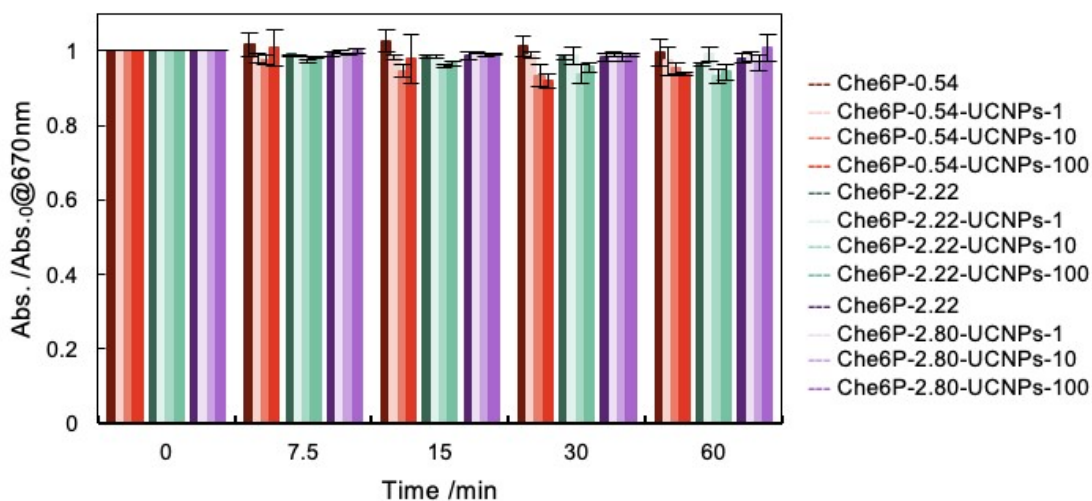
**Fig. S9** Fluorescence spectra of Che6P nanogel and Che6P-UCNPs. Che6P-0.54-UCNPs (a), Che6P-2.22-UCNPs (b), and Che6P-2.80-UCNPs (c) were dispersed in aqueous media. (Che6P,  $0.1 \text{ mg}\cdot\text{mL}^{-1}$ ; UCNPs, 1, 10, and  $100 \mu\text{g}\cdot\text{mL}^{-1}$ ). The samples were excited at 400 nm.



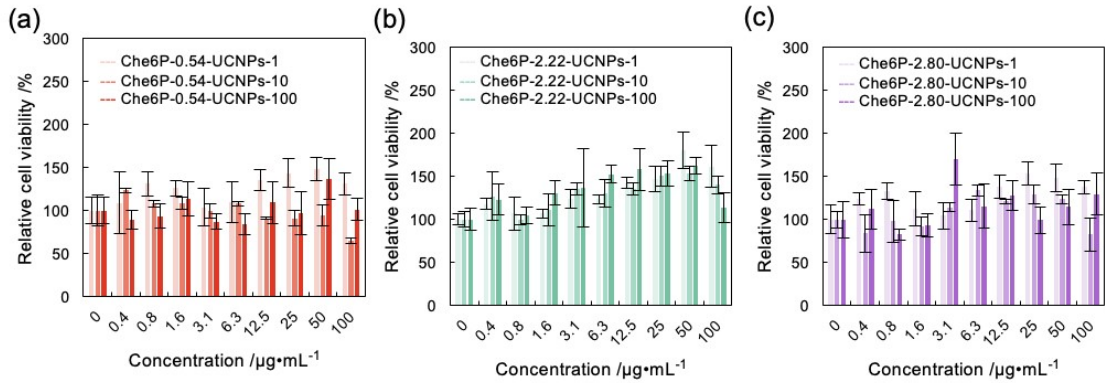
**Scheme S2** Conversion of 9,10-anthracenediyl-bis(methylene) dimalonic acid (ABDA) to endoperoxide through oxidation with singlet oxygen.



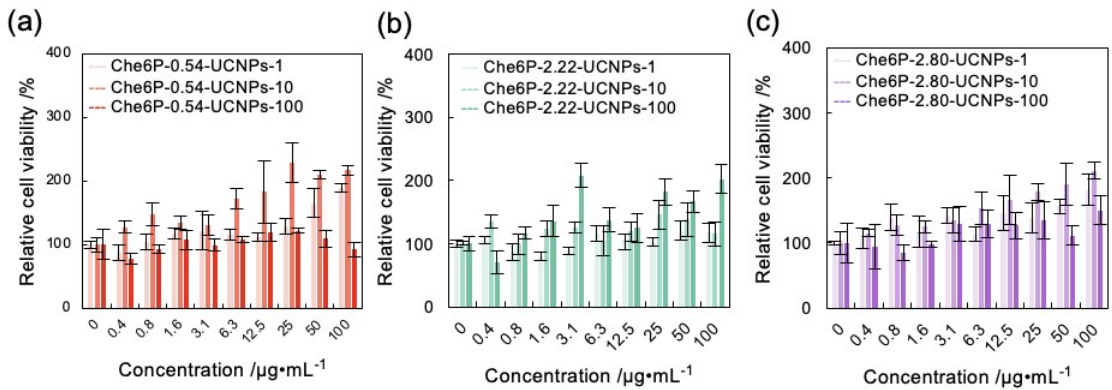
**Fig. S10** Spectral changes of 9,10-anthracenediyl-bis(methylene) dimalonic acid via photodynamic activity using (a) Che6P-0.54, (b) Che6P-0.22, (c) Che6P-2.80, (d) Che6P-0.54-UCNPs-1, (e) Che6P-2.22-UCNPs-1 (f) Che6P-2.22-UCNPs-1, (f) Che6P-2.80-UCNPs-1, (g) Che6P-0.54-UCNPs-10, (h) Che6P-2.22-UCNPs-10, (i) Che6P-2.80-UCNPs-10, (j) Che6P-0.54-UCNPs-100, (k) Che6P-2.22-UCNPs-100, and (l) Che6P-2.80-UCNPs-100. Polymer concentration was fixed at  $0.1 \text{ mg}\cdot\text{mL}^{-1}$  and the samples were exposed to 980 nm laser.



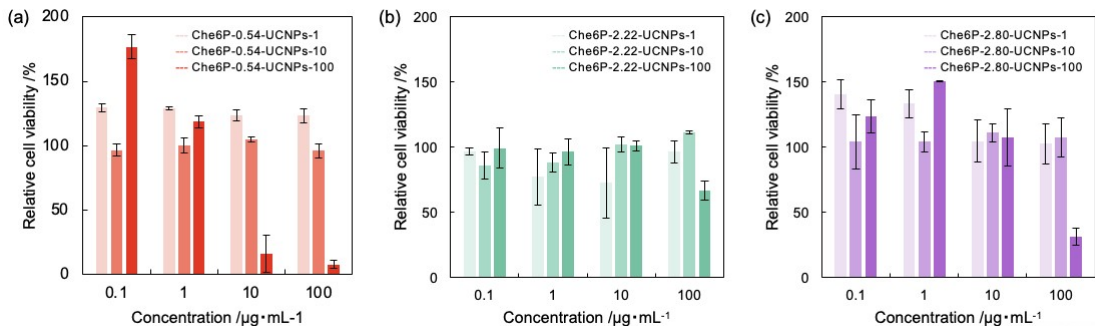
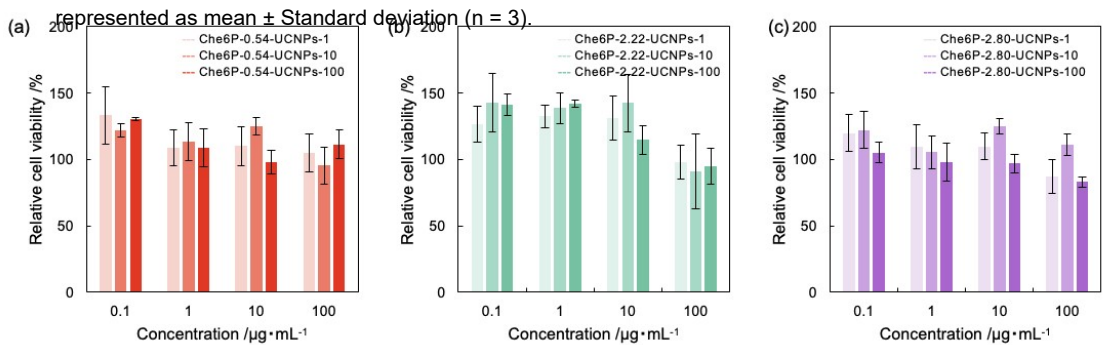
**Fig. S11** Stability of Che6P and Che6P-UCNPs against 980 nm laser exposure. Polymer concentration was fixed at  $0.1 \text{ mg}\cdot\text{mL}^{-1}$  and the samples were exposed to 980 nm laser.



**Fig. S12** Cytotoxicity of Che6P-UCNPs toward murine fibroblast (L929) in dark condition. (a) Che6P-0.54-UCNPs, (b) Che6P-2.22-UCNPs, and (c) Che6P-2.80-UCNPs were exposed to L929 with various concentration for 24 h under dark condition. The cell viability was estimated by WST-8 assay. Data represented as mean  $\pm$  Standard deviation (n = 3).



**Fig. S13** Photo-induced cytotoxicity of Che6P-UCNPs toward L929. (a) Che6P-0.54-UCNPs, (b) Che6P-2.22-UCNPs, (c) Che6P-2.80-UCNPs, were exposed to L929 with various concentration for 24 h under dark condition. Afterward, the cells were irradiated with NIR laser. The cell viability was estimated by WST-8 assay. Data



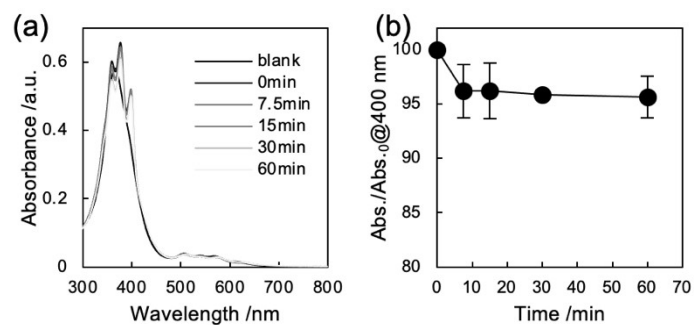


**Fig. S16** Photodynamic activity of Photofrin under 980 nm laser irradiation. (a) Spectral changes of ABDA via photodynamic activity using Photofrin. (b) Time course of ABDA bleaching through oxidation by  $^1\text{O}_2$ . Data represented as mean  $\pm$  Standard deviation ( $n = 3$ ).

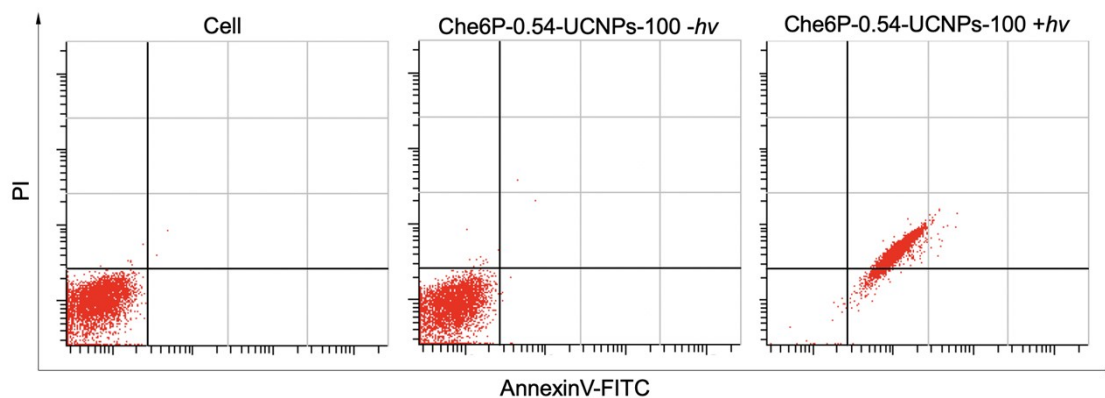


**Fig. S17** Cell apoptosis assay using Annexin V and PI. (Upper right quadrant, late apoptosis or necrosis; bottom right quadrant, early apoptosis; bottom left quadrant, live cells).

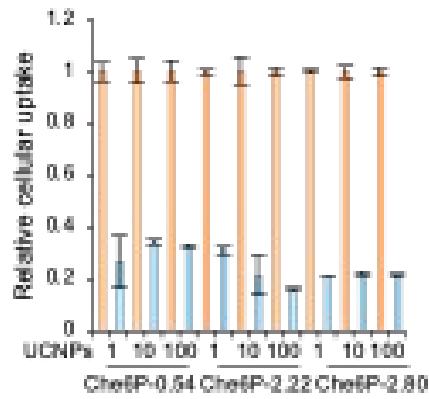


**Fig. S18** Comparison in cellular uptake of Che6P-UCNPs to Colon26 and L929. Colon26 cells (red) or L929 (blue) were treated with Che6P-UCNPs for 24 h and cellular uptake were quantified by flow cytometry. Data represent mean  $\pm$  SD (n = 3).

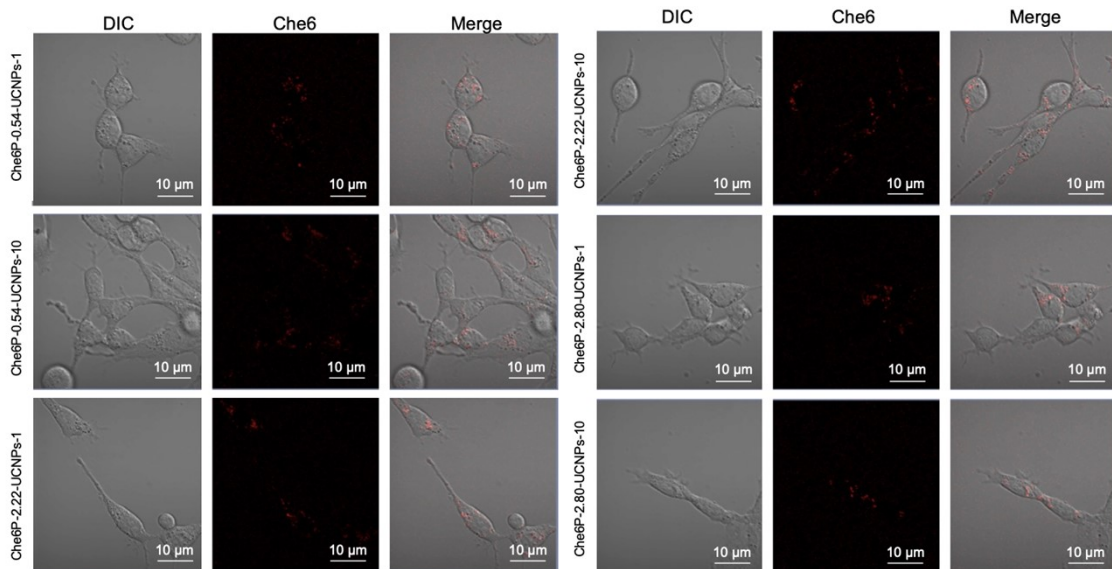


**Fig. S19** Subcellular distribution of Che6P-UCNPs. Colon26 cells were exposed to Che6P-0.54-UCNPs-100 (polymer concentration,  $0.1 \text{ mg}\cdot\text{mL}^{-1}$ ) for 24 h. The sample were observed by CLSM.

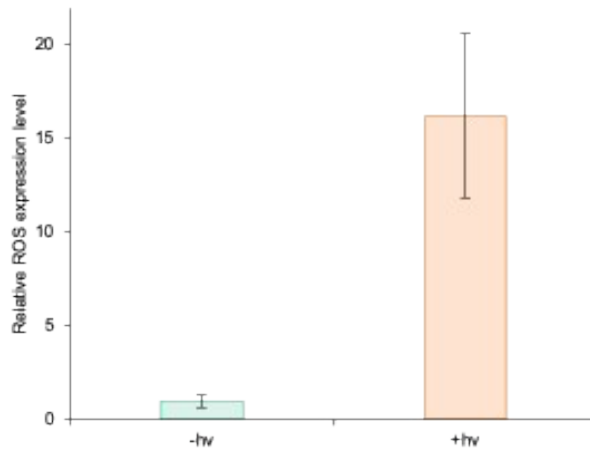


**Fig. S20** ROS expression level in Colon26 cells. Colon26 cells were exposed to Che6P-0.54-UCNPs-100 for 24 h. The cells were treated with (red) or without (blue) laser irradiation and ROS level within cells were quantified using fluorescent probe by

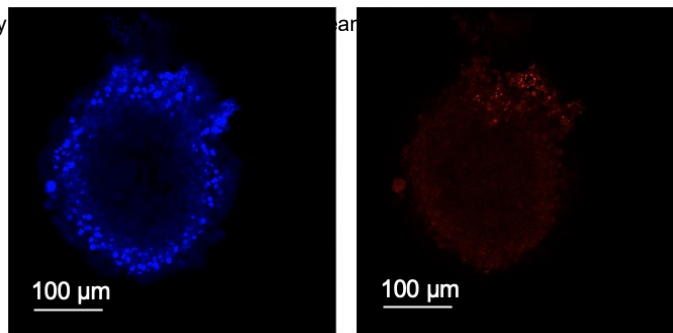


**Fig. S21** Deliverability of hybrid liposomes in Colon26 spheroid. Cellular nuclei was stained with DAPI (blue) and hybrid liposomes were visualized by chlorin e6 (red).

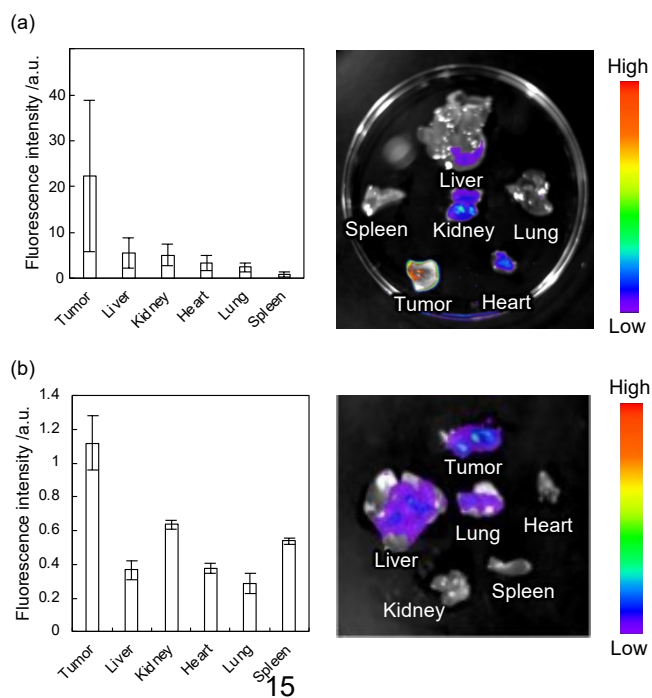


**Fig. S22** Biodistribution of Che6P-0.54-UCNPs-100. At 24 h-post injection of Che6P-0.54-UCNPs-100 ( $0.1 \text{ mg}\cdot\text{mL}^{-1}$ ,  $100 \text{ }\mu\text{L}$ ), each organ (liver, spleen, kidney, lung, tumor, and heart) was isolated and accumulation was visualized by *in vivo* imaging system (Ni

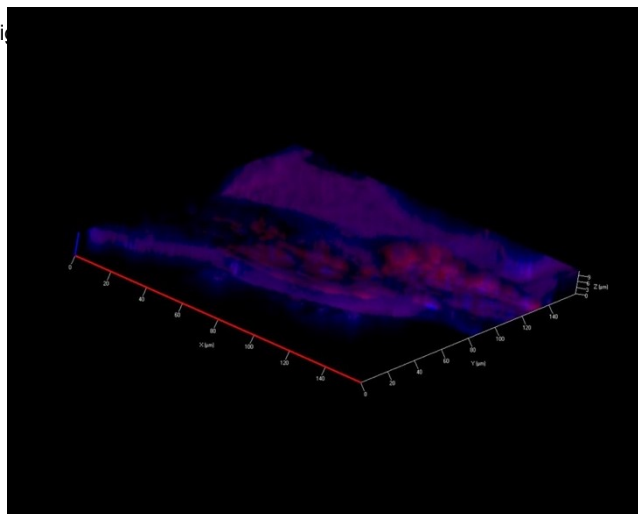


**Fig. S23** Intratumoral distribution of Che6P-0.54-UCNPs-100. At 24 h-post injection of Che6P-0.54-UCNPs-100 ( $0.1 \text{ mg}\cdot\text{mL}^{-1}$ ,  $100 \text{ }\mu\text{L}$ ), tumor was isolated and nuclei was stained with DAPI after fixation and permeabilization using 0.1 % PBST. (Red, Che6P-0.54-UCNPs-100; blue, nuclei).

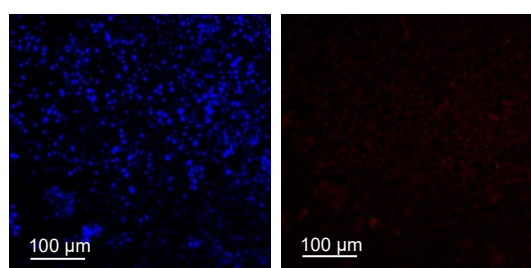


**Fig. S24** Intratumoral distribution of hybrid liposomes. At 24 h-post injection of Che6P-0.54-UCNPs-100 ( $0.1 \text{ mg}\cdot\text{mL}^{-1}$ ,  $100 \text{ }\mu\text{L}$ ), tumor was isolated and nuclei was stained with DAPI after fixation and permeabilization using 0.1 % PBST. (Red, Che6P-0.54-UCNPs-100; blue, nuclei).

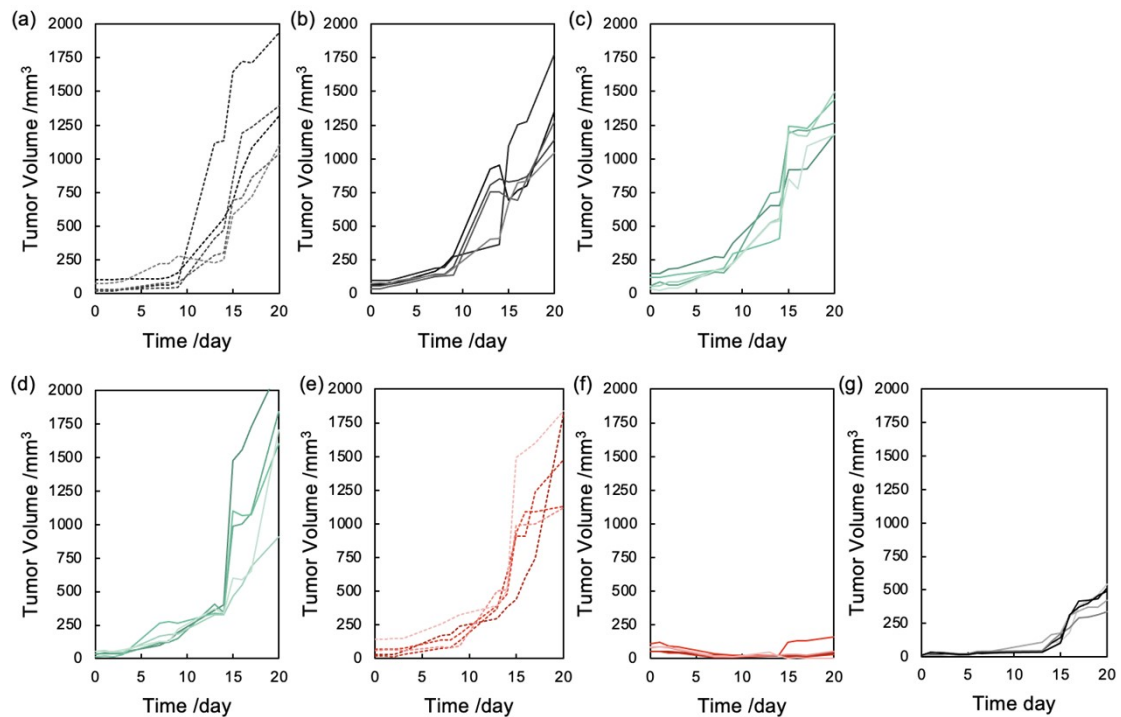


**Fig. S25** Tumor growth curve after treatment with (a) PBS *hv*<sup>-</sup>, (b) Photofrin *hv*<sup>-</sup>, (c) Che6P-0.54-UCNPs-100 *hv*<sup>-</sup>, (d) PBS *hv*<sup>+</sup>, (e) Photofrin *hv*<sup>+</sup>, or (f) Che6P-0.54-UCNPs-100 *hv*<sup>+</sup> (g) hybrid liposomes *hv*<sup>+</sup>. Each line represents the tumor growth curve for each individual in the group.

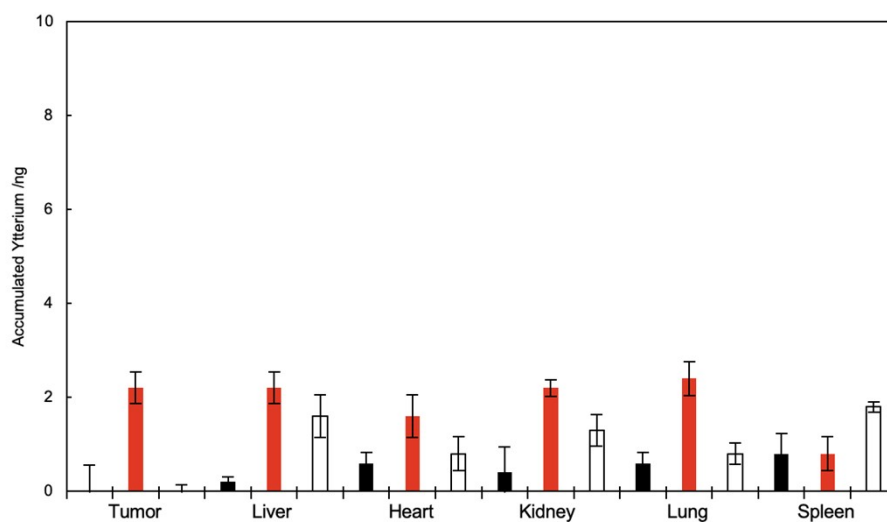


**Fig. S26** Accumulated Ytterium in each organ at 20 days-post-injection. accumulation of Ytterium using Che6P-0.54-UCNPs-100 (red) or hybrid liposomes (white) in each organ was quantified by ICP-AES. In addition, back ground level of Ytterium in each organ was also addressed (black). Data shown are mean  $\pm$  SE (n = 5).

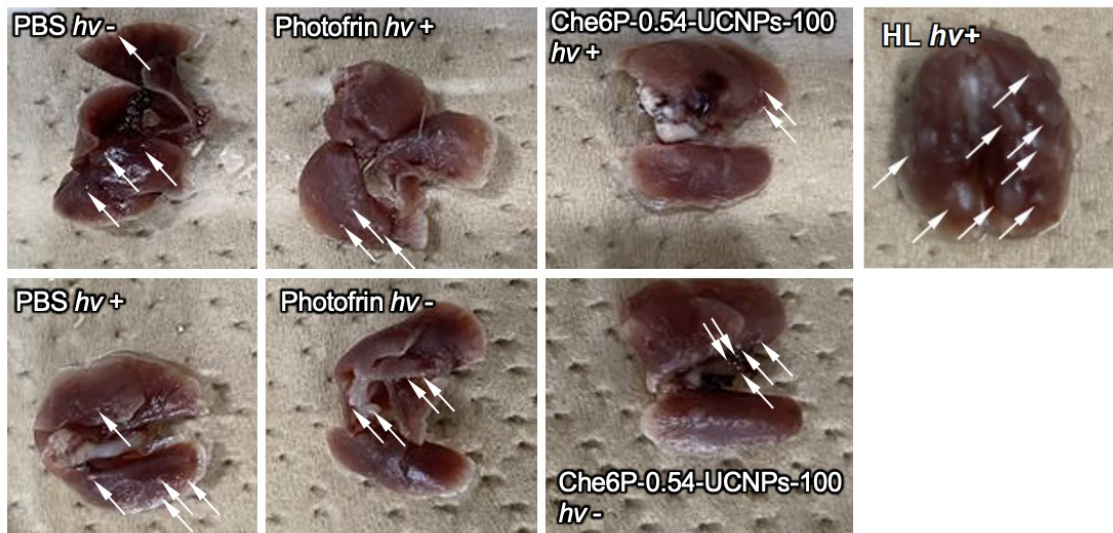


**Fig. S27** Representative images of metastatic cancer in lung. White arrows indicate the metastatic site.